

A Novel Spike Transformer Network for Depth Estimation from Event Cameras via Cross-modality Knowledge Distillation

Xin Zhang¹, Liangxiu Han^{1,*}, Tam Sobeih¹, Lianghao Han², and Darren Dancey¹

¹Department of Computing, and Mathematics, Manchester Metropolitan University, Manchester M15 6BH, UK;

²Department of Computer Science, Brunel University, Uxbridge UB8 3PH, UK

*l.han@mmu.ac.uk

ABSTRACT

Depth estimation is crucial for interpreting complex environments, especially in areas such as autonomous vehicle navigation and robotics. Nonetheless, obtaining accurate depth readings from event camera data remains a formidable challenge. Event cameras operate differently from traditional digital cameras, continuously capturing data and generating asynchronous binary spikes that encode time, location, and light intensity. Yet, the unique sampling mechanisms of event cameras render standard image based algorithms inadequate for processing spike data. This necessitates the development of innovative, spike-aware algorithms tailored for event cameras, a task compounded by the irregularity, continuity, noise, and spatial and temporal characteristics inherent in spiking data. Harnessing the strong generalization capabilities of transformer neural networks for spatiotemporal data, we propose a purely spike-driven spike transformer network for depth estimation from spiking camera data. To address performance limitations with Spiking Neural Networks (SNN), we introduce a novel single-stage cross-modality knowledge transfer framework leveraging knowledge from a large vision foundational model of artificial neural networks (ANN) (DINOv2) to enhance the performance of SNNs with limited data. Our experimental results on both synthetic and real datasets show substantial improvements over existing models, with notable gains in Absolute Relative and Square Relative errors (49% and 39.77% improvements over the benchmark model Spike-T, respectively). Besides accuracy, the proposed model also demonstrates reduced power consumptions, a critical factor for practical applications.

1 Introduction

Event-based cameras are bio-inspired sensors that capture visual information asynchronously, reporting brightness changes in real-time^{1,2}. Unlike traditional cameras, the major advantages of event-based sensors include low latency between triggered events³, low power consumption⁴ and high dynamic range⁵. These benefits come directly from the hardware design, and event-based cameras have been used in a variety of fields such as 3D scanning⁶, robotic vision⁷, and automotive industry⁸. However, in practice, the event-based sensor captures unique spike data that encodes information of light intensity changes in a scene. The noise in the data is extremely high and there is a lack of generalized processing algorithms for these data to provide comparable capabilities similar to traditional vision algorithms for data from conventional digital camera.

Spiking Neural Networks (SNNs) are bio-inspired neural network models that mimic the behaviour of biological neural networks. SNNs use discrete functions called spikes to represent and process information, as opposed to continuous values used in traditional vision algorithms⁹. Therefore, it is naturally an ideal paradigm for processing the output of event cameras^{10–12}.

Depth estimation is a challenging task in computer vision, which are widely used in autonomous driving, automated robotics, agricultural growth monitoring, and forest carbon emission monitoring. Current state-of-the-art depth prediction efforts have mainly focused on combining standard frame-based cameras with artificial neural networks (ANN)^{13–15}. However, event-based cameras and associated processing algorithms for depth-sensing applications are still at an infancy stage⁵. A number of challenges remain, including lack of SNN backbone for feature extraction and poor SNN model performance, are two major issues.

Lack of SNN backbone designed for spike data depth estimation. The event-based camera generates continuous spike streams in a binary irregular data structure that possesses ultra-high temporal features. SNN is applicable to event camera datasets and able to improve the depth estimation performance by exploiting advanced architecture of ANN, such as ResNet-like SNNs and Spiking Recurrent Neural network^{16–19}. Vision transformer^{20,21} (ViT) which is based on self-attention mechanism to capture long-distance dependencies, especially spatial-temporal features in images/videos, is currently the most popular ANN structure. It improves the performance of AI in many computer vision tasks such as image classification/segmentation^{2,22},

object detection²³ and depth estimation^{24,25}. Transformer-based SNNs are a kind of new form of SNNs that combine transformer architectures with SNNs, offering great potential to break the performance bottleneck of SNNs on spike stream data. In²⁶, the authors used the original ViT structure as a backbone to extract features from both spatial and temporal domains in spike data. The result demonstrated the suitability of the transformer for extracting spatio-temporal features in spike data. However, the original transformer structure has a large number of multiplication operations and has excessive computational energy consumption compared to SNNs. In²⁷ and²⁸, the author proposed a pure spike driving self-attention and residual connection to avoid non-spike computations in transformer. This pushes a major step forward for the potential use of transformer for the depth estimation from spike data.

SNN model performance. One of the biggest challenges with SNNs currently is their inability to achieve an equivalent performance on spiking data like ANNs do on non-spiking data. The spiking data is non-differentiable, which makes it difficult to use the backpropagation algorithm to train SNNs. Gradient-based Backpropagation is a powerful algorithm for training ANNs, but it cannot be used directly with SNNs²⁹. Converting ANN to SNN directly is a solution but it may introduce errors of uncertainty or lose temporal information of spikes¹⁹. Meanwhile, the event-based datasets are small compared to the static images used in traditional ANN training, making SNNs prone to overfitting and limits their generalization ability²⁹. Knowledge distillation is a technique in deep learning by transferring knowledge from the teacher model to the student model. It allows to train a lightweight model (student model) to be as accurate as a larger model (teacher model). Currently, there are already some ANN models trained with massive data that can achieve zero-shot for depth estimation³⁰⁻³². These models logically have the potential to be transferred to the SNN model training.

In this work, by leveraging the unique biological properties of SNNs and the advanced cross-modality knowledge distillation from a visual foundation model(DINOv2), we propose a spike-driven transformer for depth estimation via cross-modality knowledge distillation. To the best of our knowledge, this is the first exploration of transformer based SNN for depth estimation. We highlight three main contributions of our study as follows:

1. We introduce an innovative spike transformer network specifically designed for depth estimation. This network incorporates spike-driven residual learning and spike self-attention mechanisms to eliminate the need for floating-point and integer-float multiplications, adhering to the principled spike-based operation. This approach significantly reduces energy consumption while ensuring robust performance.
2. We develop a comprehensive single-stage knowledge distillation framework, deriving insights from both the final and intermediate layers of the large vision foundation ANN model (DINOv2). Utilizing domain loss and semantic loss, our framework effectively transfers knowledge to the SNN, facilitating the efficient training on limited datasets.
3. We have conducted thorough experimental evaluation by comparing the proposed approach with the state-of-the-art methods on both real and synthetic datasets. The results demonstrate that our proposed method reliably predicts depth maps and outperforms competing methods by a significant margin.

2 Related works

This section covers related works in image and event based Monocular depth estimation, Spiking Neural Networks (SNNs) and Knowledge distillation for SNN.

2.1 Image-based and Event-based Monocular Depth Estimations

Depth estimation from images aims to measure the distance of each pixel relative to the camera. Monocular depth estimation, i.e. based on a single image, is a challenging but promising technology. It has the advantage of not requiring two images, which makes it more practical for applications where it is not possible to take a pair of images, such as mobile devices. Depending on the type of data used, we can divide the monocular depth estimation method into Image-based and Event-based methods¹⁴. The Image-based monocular depth estimation uses the information in an RGB image to estimate depth, while the event-based method uses the spike data generated by event camera. Image-based monocular depth estimation is more common than event-based monocular depth estimation because RGB images are easier to collect and process. Event cameras are a new type of sensors that output brightness changes in the form of an asynchronous "event" stream, rather than static images. This makes them well-suited for depth estimation in challenging conditions, such as low light and fast motion³³.

The latest developments in deep learning have made it possible to develop monocular depth estimation models that can achieved satisfactory accuracy and robustness^{14,34,35}. Similar to other deep learning models, these models typically consist of a generalized encoder that extracts abstract features from context information and a decoder that recovers depth information from the features. For RGB images, in³⁶, the author used ResNet-50 as an encoder and a novel up-sampling blocks as a decoder to estimate depth from a single RGB image. In³², the authors utilised ViT instead of convolutional networks as the backbone for a depth estimation task. Experiments have found that transformer is able to provide finer and more globally consistent

predictions than traditional convolutional networks. For event data, the authors³³ presented a new deep learning model called E2Depth that can estimate depth from event cameras with high accuracy. A fully convolutional neural network based on the U-Net architecture³⁷ were used in this work. In³⁸, a multiscale encoder was used to extract features from mixed-density event stacking and an upscaling decoder was used to predict the depth. The transformer structure was also used in event-based monocular depth estimation. In³⁹, EReFormer was proposed to estimate depth from event cameras with superior accuracy based on transformer.

Traditional deep learning relies on supervised learning, which typically requires large amounts of training data. Especially for transformer architectures, which can learn long-range dependencies and have a tremendous demand for data²¹. For monocular depth estimation, with massive training data, the performance of the model can be improved³². The requirement for large data training significantly limits the scalability and usability of the model. Moreover, it is almost impossible to train a deep learning model in a supervised manner on the spike data stream because it is too time-dense to obtain paired depth labels.

In response to these challenges, self-supervised learning, Un-supervised learning, and knowledge distillation have emerged as new hotspots for deep learning model training on spiking data. Self/Un-supervised learning is a type of machine learning where the model learns from unlabelled data, while Knowledge distillation is a technique that transfer knowledge from large, trained model to a new model. It is reasonable to expect that these techniques have potential to be utilised in event-based monocular depth estimation. In the paper³⁹, the author distilled the knowledge from large trained models to improve the performance of the proposed model.⁴⁰ proposed an unsupervised spike depth estimation method via knowledge transfer from an image-based depth estimation model.

2.2 Spiking Neural Networks (SNNs)

Unlike traditional deep learning models that convey information using continuous decimal values, SNNs use discrete spike sequences to calculate and transmit information. Spiking neurons receive continuous values and convert them into spike sequences. A number of different spiking neuron models have been proposed. Hodgkin-Huxley model is one of the first models that describes the behaviour of biological neurons⁴¹, which is a fundamental model to explain how spike flows in neurons, but the model is too complex to implement in silicon. Lzhikevich model⁴² simplified Hodgkin-Huxley model, which is a two-dimensional model that describes the dynamics of the membrane potential of a neuron. The leaky integrate-and-fire (LIF) neuron is another simple model of a neuron that is widely used in neuroscience and artificial neural networks. It is simpler than Lzhikevich model but captures the essential features on how neurons work. It can be used to build SNN and implemented in very-large-scale integration (VLSI)[5]. The membrane potential of the LIF neuron is governed by the following equation:

$$dv/dt = I - v/\tau \tag{1}$$

where v is the membrane potential, t is time, τ is a time constant, and I is the current. The current, I , can be either excitatory or inhibitory. Excitatory currents make the membrane potential more positive, while inhibitory currents make it more negative. When the membrane potential reaches the threshold, the neuron fires an action potential. In this work, LIF is used to build the proposed model.

In the SNN structure design, similar to ANN, as the depth of spiking neural networks (SNNs) increases, their performances have been significantly improved^{16,17,43}. Currently, most SNNs have borrowed structures from ANNs, which can be categorized into two main groups: CNN-based SNNs and transformer-based SNNs.

ResNet, as the most successful CNN model has been extensively studied to extend the depth of SNNs^{16,17}. SEW ResNet¹⁶ overcomes the vanishing/exploding gradient problem in SNNs by using a technique called spike-timing-dependent plasticity (STDP). It has been shown effective in a variety of tasks, including image classification and object detection. However, Convolutional networks possess translation invariant and locally dependent, but their calculation has a fixed receptive field, limiting their ability to capture global dependence. In contrast, ViT is based on self-attention mechanisms that can capture long-distance dependencies. They are based on the Transformer architecture, which was originally developed for natural language processing tasks.

Transformer-based SNNs represent a novel form of SNNs that combines the transformer architecture with SNNs, providing great potential to break through the performance bottleneck of SNNs.

In Yao et al.⁴⁴, and Zhou et al²⁷, proposed two different Spike-Driven Self-Attention models. They utilised only mask and addition operations to avoid multiplication, which are efficient and have low computational energy consumption. Zhou et al²⁸, proposed Spikingformer, which modified the residual connection to purely event-driven, which is energy efficient while improving performance.

Currently, ViTs have been shown to achieve state-of-the-art results in a variety of vision tasks, including image classification, object detection, segmentation and depth estimation. However, the transformer based SNNs is still in its infancy in depth estimation²⁶. There are two major issues: 1) the difficulty in training pure transformer based SNN models; 2) and the

limited availability of paired depth data in event data to support transformer model training. Knowledge distillation provides a manner to train new or small models using well pretrained models. In this work, we propose a knowledge distillation method to bring ANN model knowledge into SNN.

2.3 Knowledge distillation for SNN

Knowledge distillation is a type of model compression techniques that transfers knowledge from large teacher models to smaller student models. It has gained attention due to its ability to train deep neural networks using limited resources⁴⁵. Meanwhile, knowledge distillation has been shown effective in improving the performance of SNNs. In⁴⁶, the author proposed a knowledge distillation method for transferring knowledge from a large trained SNN to a small one in an image classification task. The results show that using the knowledge of pre-trained large models can significantly improve the performance of small models, thus enhancing the possibility of deploying high-performance models on resource-limited platforms. In study²⁹, a knowledge distillation method was proposed for SNNs for image classification. The method was able to improve the accuracy of a student SNN by up to 2.7% to 9.8% by introducing knowledge distillation. The authors⁴⁷ found that the knowledge distillation paradigm can be effective in reducing the performance gap from the ANN to the SNN. The distillation between ANNs and SNNs using similar structures improved the model performance. In [42], knowledge distillation was first used for depth estimation of SNNs. The author proposed a cross-modality domain knowledge transfer method for unsupervised spike depth estimation with open-source RGB data.

However, existing knowledge distillation methods for SNNs all require training a teacher model first. Currently, large foundation models become the new deep learning hotspot⁴⁸. A large foundation model is trained on a vast quantity of data at scale (often by self-supervised learning or semi-supervised learning) so that the learned features can be used directly for various downstream tasks or knowledge distillation. For example, Dense Prediction Transformers (DPT)³² are a type of ViT that is designed for depth prediction tasks, which was trained on 1.4 million images for monocular depth estimation. DINOv2³⁰ used ViT-Giant, a larger version of ViT with 1 billion parameters. It is more powerful than previous ViT models and outperforms previous self-supervised learning methods in a variety of computer vision tasks, especially for depth estimation. In this work, for the first time, we will explore to transfer knowledge from a large foundation model (DINOv2)³⁰ to SNNs for depth estimation.

3 The Proposed Method

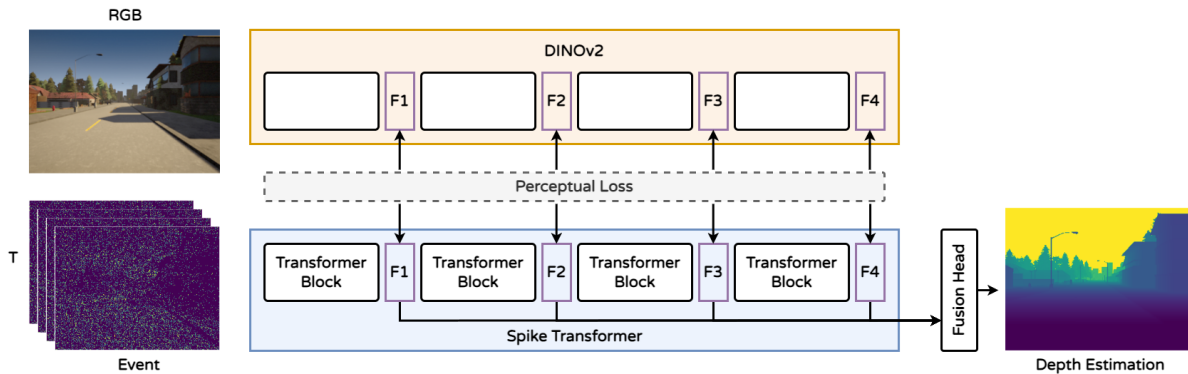


Figure 1. The flowchart of the proposed method

We introduce a novel pure spike-based transformer computational network for depth estimation via cross-modality knowledge distillation. The network architecture employs an encoder-decoder structure, with the transformer serving as the core computational unit of the encoder. A fusion decoder is specifically crafted to amalgamate features from different stages of the encoder, thus producing a comprehensive depth map. The flowchart of the method is illustrated in Figure 1, encompassing three primary components: 1) Spike-driven transformer, 2) Knowledge distillation, and 3) Fusion depth estimation head.

The underpinnings of our proposed methodology are outlined as follows:

1. Transformers, renowned for their capability to capture long-range dependencies through self-attention and matrix multiplications, typically require computationally intensive operations that are not well-suited for the spike-driven paradigm. In this context, we introduce a pure spike-driven transformer network that leverages spike-driven residual learning and spike self-attention. This design eschews conventional floating-point and integer-float multiplications, adhering strictly to spiking principles and thus achieving substantial energy savings while maintaining robust performance.

2. SNNs are energy-efficient models that use binary spikes instead of continuous values, but they also need deep architectures to achieve high accuracy, which can be computationally expensive and power-hungry. Knowledge distillation allows leveraging the knowledge of a pre-trained ANN (teacher) to guide the training of a smaller SNN (student) model, enabling it to achieve similar performance with fewer resources. In this work, a cross-modality knowledge distillation method is proposed between RGB and event data. The proposed method is trained through matching RGB and event data, while the inference is performed on event data only. The large pretrained vision foundation model DINOv2 is used as the teacher model for knowledge distillation, which does not participate in training and only extracts features from the RGB data.
3. Differing from conventional fully convolutional networks that employ downsampling, transformer networks maintain consistent dimensional representations, facilitating global receptive fields essential for tasks such as segmentation or depth prediction. Hence, we propose a fusion depth estimation head capable of harnessing features from each transformer stage to optimize depth estimation effectiveness.

3.1 Pure spike-driven transformer network for depth estimation

In this work, we propose a pure spike transformer-computational network for depth estimation via cross-modality knowledge distillation. The design of the proposed method follows a pattern that logically divides the network into an encoder and a decoder. The spike-transformer block is selected as the encoder to extract spatial-temporal features from spike data. A fusion depth estimation head is designed as the decoder to generate pixel-scale depth results from the feature representation.

3.1.1 Spike-transformer

The proposed spike transformer aligns with the foundational structure of the original Vision Transformer (ViT), encompassing a Spiking Patch Embedding and Spiking Transformer Block. Given an event sequence. $I \in \mathbb{R}^{T \times C \times H \times W}$, the spike patch embedding is used to convert the input into a sequence of tokens that can be processed by the transformer architecture, where the event input is projected as spike-form patches $X \in \mathbb{R}^{T \times N \times D}$, $N = \frac{H}{8} \times \frac{W}{8}$. Then, the spiking patches X are passed to the multi spiking transformer blocks (L). Considering that we have used knowledge distillation from the large model, this method uses only a minimum number of blocks as $L = 4$. Inspired by^{27,28}, in order to avoid non-spike computations in traditional deep learning architectures, a Spiking Self Attention (SSA) and a Spiking MLP block are used in spiking transformer blocks.

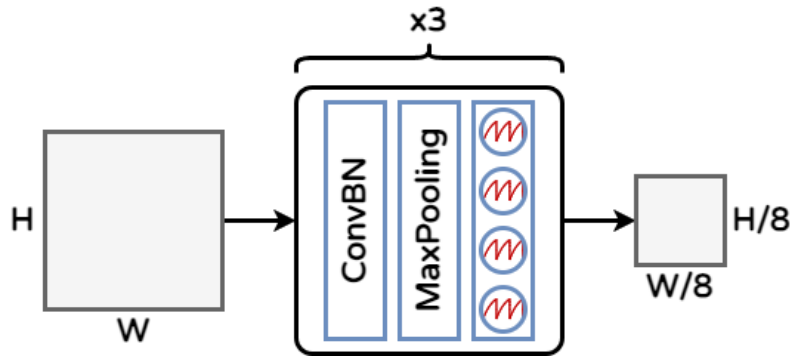


Figure 2. The structure of spiking patch embedding

Spiking patch embedding In the original ViT²⁰, the patch embedding is used to represent an image as a sequence of tokens. This is done by dividing the image into a grid of patches and flattening each patch into a vector. In this work, we implement this operation through a convolution batch norm (ConvBN), Max pooling (MP) and multistep LIF (MLIF) combination. The structure is shown in Figure 2. This process can be formulated as:

$$I_i = \text{MLIF}(\text{MP}(\text{ConvBN}(I))) \quad (2)$$

where the *ConvBN* contains 2D convolution layers (stride-1, 3×3 kernel size) and max-pooling. The number of operations can be bigger than 1. When multiple blocks are used, the number of output channels gradually increases and the size of the feature is halved, eventually matching the embedding dimension of the patch in ViT.

Spiking Transformer Block The Spiking Transformer Block is structured to incorporate both a Spiking Self Attention (SSA) mechanism and a Spiking MLP block, as illustrated in Figure 3.

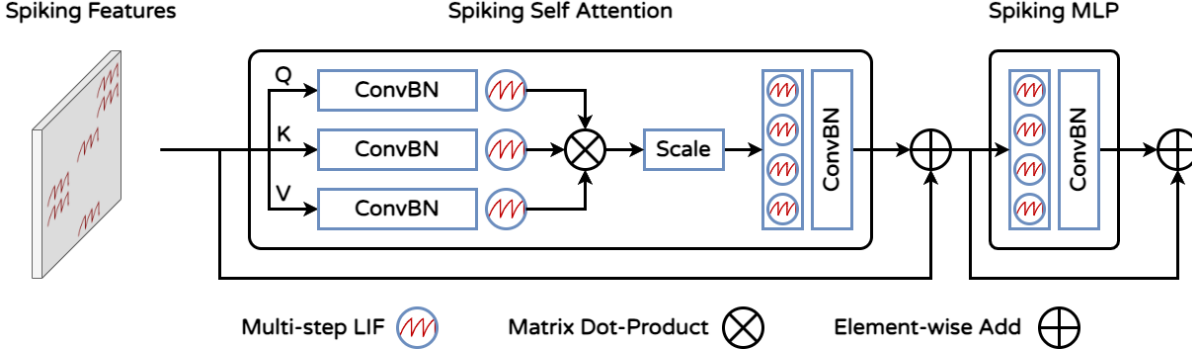


Figure 3. The structure of transformer block

Guided by the findings in²⁸, we position a multistep LIF before the ConvBN within the residual mechanism to omit floating-point multiplication and mixed-precision calculations during the ConvBN operation. This adjustment also enables ConvBN to replace conventional linear layers and batch normalization seamlessly. The SSA operation can be mathematically described as:

$$\begin{aligned}
 Q &= \text{MLIF}_Q(\text{ConvBN}_Q(X')) \\
 K &= \text{MLIF}_K(\text{ConvBN}_K(X')) \\
 V &= \text{MLIF}_V(\text{ConvBN}_V(X')) \\
 \text{SSA}(Q, K, V) &= \text{ConvBN}(\text{MLIF}(QK^T V * s))
 \end{aligned} \tag{3}$$

The variables $Q, K, V \in \mathbb{R}^{T \times N \times D}$ represent pure spike data (only containing 0 and 1). The Scaling factor, s , is used to adjust the largest value of the matrix multiplication result. It does not affect the property of SSA. The Spiking MLP block consists of a residual connection and a combination of MLIF and ConvBN.

3.1.2 Fusion Depth estimation Head

The aim of depth estimation head is to predict the depth for each pixel which is similar to the segmentation task. The most dominant segmentation framework currently is the U-Net based multiscale structure. The decoder of U-Net uses skip connections from layers of different scale in the encoder to help preserve the spatial information of input images. This helps to ensure that the decoder has access to both the low-level and high-level features from the encoder, in which the low-level features are important for capturing details and the high level features are important for understanding the overall structure of the image. Unlike traditional CNN structures, the size of hidden features in the transformer structure is invariant and it is not straightforward to use the U-Net structure. There are a number of models that use transformer as the backbone for segmentation and redesign the structure of the transformer, such as Multiscale vision transformers⁴⁹, Pyramid vision transformer⁵⁰, Multi-Path Vision Transformer⁵¹, etc. In this work, a knowledge distillation is selected to distil the knowledge from the trained large transformer into the proposed SNN. Modifying the structure will significantly reduce the effectiveness of the distillation. Therefore, a fusion depth estimation head is proposed to predict the depth.

The structure of the fusion head for depth estimation is shown in Figure 4. The first step of the fusion head is to assemble the internal features in transformer blocks into image-like feature representations. The feature representations are then fused into the final dense prediction with skip connections. A generic up sample structure is used to restore the feature representations to original data size. Give an input feature as $F_i \in \mathbb{R}^{T \times H/8 \times W/8}$, $i=1,2,3,4$. The depth estimation head can be formulated as follows:

$$\begin{aligned}
 Y &= \text{ConvBn}(Up(\text{ConvBn}(\text{ConvBn}(\text{ConvBn}((\text{ConvBn}(Up(F_1)) + Up(F_2)) \\
 &\quad + Up(F_3)) + Up(F_{i+4})))))) \\
 Y &= \text{Sigmod}(Y)
 \end{aligned} \tag{4}$$

3.2 Knowledge distillation from DINOv2

In this work, a method of cross-modality knowledge distillation is outlined, wherein a large-scale vision foundation model, specifically DINOv2, is utilized to guide the training of our SNN. The DINOv2 model, trained on a diverse dataset comprising 142 million images³⁰, is advantageous for several reasons:

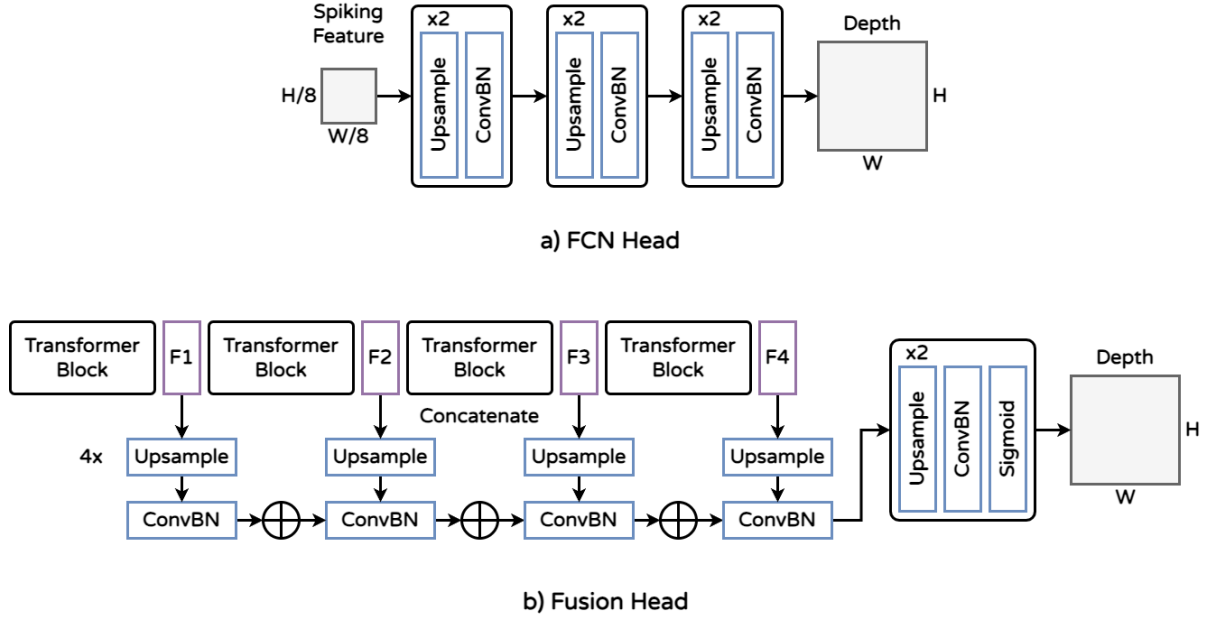


Figure 4. The structure of the fusion head for depth estimation.

1. The architecture of DINOv2, based on the Vision Transformer (ViT), resembles that of our model, facilitating effective knowledge distillation owing to their structural and feature-size compatibility.
2. The features extracted from the DINOv2 pre-trained model have been used to achieve the state-of-the-art performance on the NYU and SUN RGB-D depth estimation benchmark datasets. Figure 5 shows the visualization of self-attention on DIVO_V2 features and the depth estimation result with a linear probe on frozen DINOv2 features on our dataset. The DIVNO v2's feature representations (the middle column in Figure 5) and the depth estimation result close to the real depth of the image, as visualized in the figure, supports the hypothesis that the DINO V2 model can provides effective guidance during the knowledge distillation training process.

Figure 1 shows the knowledge distillation process. We freeze the DINOv2 as a teacher model. The output features from DINOv2 are considered as targets in our training. To obtain the same feature size, we upsample the RGB image by a factor of 1.75. The final feature size of teacher model is $x_{rgb} \in \mathbb{R}^{d \times H/8 \times W/8}$.

Figure 6 shows the knowledge distillation algorithm. In our approach, we utilize a fusion loss function. The L1 loss measures the differences in features between the student and teacher networks. The Perceptual Loss⁵², a method commonly used in machine learning to quantify discrepancies between two images, is also adopted here. The L2 loss function, a scale-invariant metric⁵³, is chosen to evaluate the results of depth estimation. This scale-invariant feature ensures that the loss does not penalize the model for discrepancies arising from the scale of input data, demonstrating effectiveness for monocular depth estimation. The scale-invariant loss is defined by the following equations:

$$\mathcal{L}_1 = \frac{1}{C \times H \times W} \|x - x'\|_2^2$$

$$\mathcal{L}_2 = \frac{1}{n} \sum_{\mathbf{i}} (D_i^t - D_i^p)^2 - \frac{1}{n^2} \left(\sum_{\mathbf{p}} D_i^t - D_i^p \right)^2 \quad (5)$$

Where $D_i^t - D_i^p$ is the difference between predicted and ground truth depth for pixel \mathbf{i} , and n is total number of pixels with a dimension of $H \times W$.

4 Experiments

In this work, we conduct two experiments to demonstrate the effectiveness of the proposed SNN. We first introduce the details of datasets used in this experiment. Then, we evaluate the performance of our method, including accuracy and energy consumption.

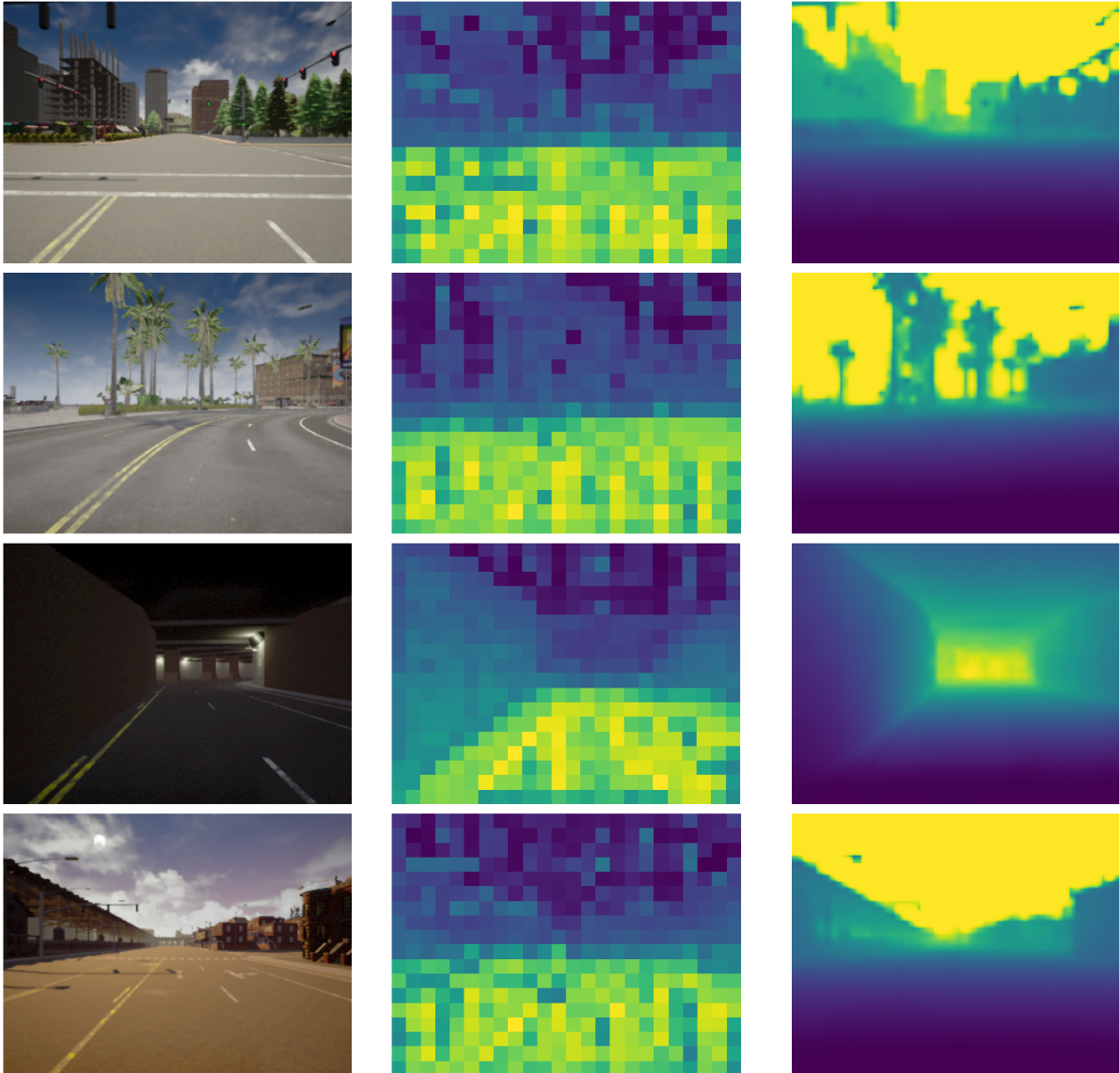


Figure 5. a) The RGB image; b) Visualization of self-attention on DINOv2 features; (c) Depth estimation results using a linear probe on frozen DINOv2 features.

Algorithm 1 Spike knowledge distillation algorithm

Input:

x_batch : One batch Spike images;
 x_{rgb_batch} : One batch Mathced RGB images;
 T : Teacher Network;
 S : Student Network;
 H : Depth estimation head Network;

- 1: set $T.params = S.params$;
- 2: set $T.Frozen()$ # Frozen Teacher’s params;
- 3: **for** x, x_{rgb} **in** x_batch, x_{rgb_batch} **do** # One batch training
- 4: $x' = T(x)$
- 5: $x'_{rgb} = S(x_{rgb})$
- 6: $D = H(x')$
- 7: $loss = L1(x', x'_{rgb})/2 + L2(D, Target)/2$
- 8: loss.backward() # Back-propagate
- 9: Update($S.params$) # Student params update by knowledge distillation
- 10: **end for**

Figure 6. The knowledge distillation algorithm

We evaluate our method on both real and synthetic event data to demonstrate the robustness and generalisability of the model. Finally, comprehensive ablation studies are conducted, which investigate the impact of each component.

4.1 Datasets

For model evaluation, we utilize two datasets comprising both real and synthetic data.

The first dataset is a synthetic dataset from²⁶, which is generated from DENSE dataset³³, including clear depth maps and intensity frames in 30 FPS under a variety of weather and illumination conditions. To obtain spike streams with high temporal resolution, the video is interpolated to generate intermediate RGB frames between adjacent 30-FPS frames. With absolute intensity information among RGB frames, each sensor pixel can continuously accumulate the light intensity with the spike generation mechanism, producing spike streams with a high temporal resolution (128×30 FPS) that is 128 times of the video frame rate. The ‘spike’ version of DENSE dataset (namely DENSE spike) contains eight sequences, five for training, and three for evaluation. Each sequence consists of 999 samples, and each sample is a tuple of one RGB image, one depth map, and one spike stream. Each spike stream is simulated between two consecutive images, generating a binary sequence of 128 spike frames (with a size of 346×260 each) to depict the continuous process of dynamic scenes.

The second dataset, DSEC, is a real event dataset that provides stereo dataset in driving scenarios. It contains data from two monochrome event cameras and two global shutter colour cameras in favourable and challenging illumination conditions. Hardware synchronised LiDAR data is also provided for depth prediction. The dataset contains 41 sequences collected by driving in a variety of illumination conditions and provides ground truth disparity for the depth estimation evaluation. In this work, 29 sequences (70%) are used for model training and 12 are used for evaluation. Each sequence consists of 200-900 samples, and each sample is a tuple of one RGB image, one depth map (dense disparity), and one spike stream with 16 spike frames and size of 480×640 . Figure 7 presents the two data samples used in this work.

4.2 Experiment design

4.2.1 Experiment 1. Qualitative and Quantitative Comparisons

In this section, we evaluate the depth estimation performance and energy consumption of our SNN on the synthetic (DENSE) and real datasets (DSEC) and compare it with three competing dense prediction networks, namely U-Net³⁷, E2Depth³³ and Spike-T²⁶. U-Net employs 2D convolutional layers as its encoder and focuses on spatial feature extraction, while E2Depth applies ConvLSTM layers that combine CNN and LSTM to capture the spatial and temporal features. The Spike-T employs

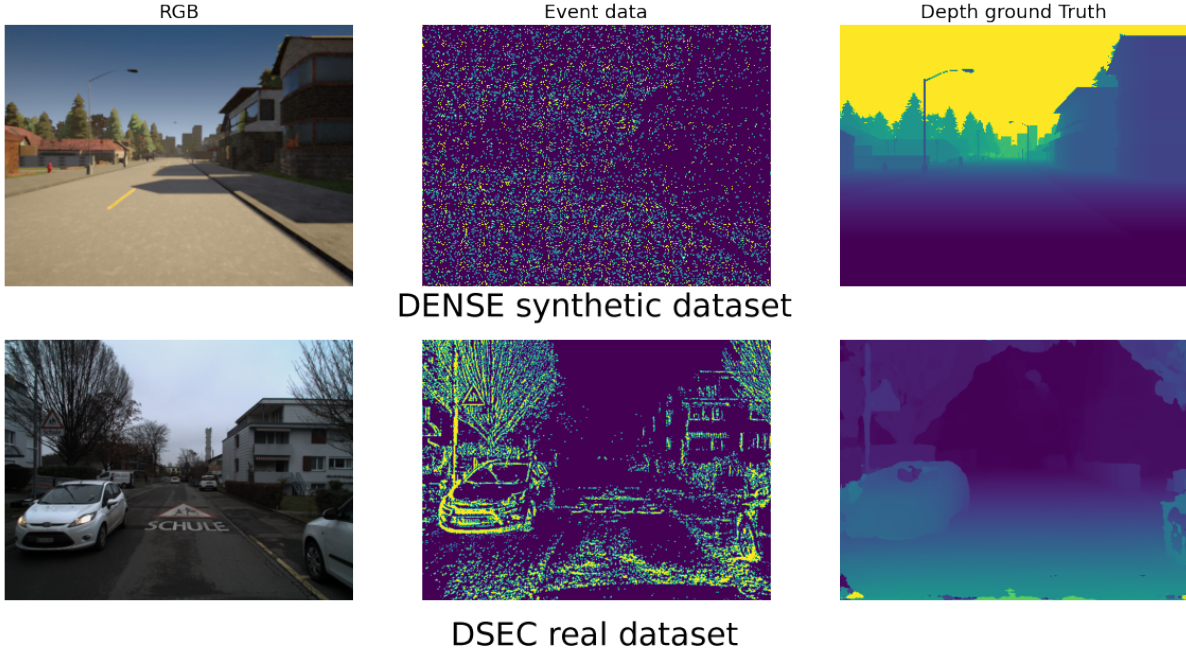


Figure 7. Showcase of the two datasets.

transformer-based blocks to learn the spatio-temporal features simultaneously. These models therefore constitute our immediate and direct competitors.

4.2.2 Experiment 2 Ablation study: the contribution of the proposed modules

An ablation study is detailed in this subsection to investigate the contributions of two novel components within our model. They are the fusion depth estimation head and the knowledge distillation technique. Their respective impacts on model performance are dissected and discussed.

4.3 Metrics

Several metrics are selected to evaluate the performance of the proposed method, including absolute relative error (Abs Rel.), square relative error (Sq Rel.), mean absolute depth error (MAE), root mean square logarithmic error (RMSE log) and the accuracy metric (Acc. δ). The formulations are as follows:

Absolute Relative Error (Abs Rel.) computes average errors on the normalized depth map for every pixel, formulated as:

$$AbsRel. = \frac{1}{N} \sum_p \frac{|\mathcal{D}_p - \widehat{\mathcal{D}}_p|}{|\mathcal{D}_p|} \quad (6)$$

It normalises the value of depth to the range [0,1].

Square Relative Error (Sq Rel.), formulated as

$$SqRel. = \frac{1}{N} \sum_p \frac{|\mathcal{D}_p - \widehat{\mathcal{D}}_p|^2}{|\mathcal{D}_p|} \quad (7)$$

which focuses on large depth errors due to its square numerator.

Mean Absolute Error (MAE) can be formulated as:

$$MAE = \frac{1}{N} \sum_p |\mathcal{D}_p - \widehat{\mathcal{D}}_p| \quad (8)$$

Root Mean Square Error (RMSE) is a classic metric for per-pixel prediction error and the logarithm version can be denoted as

$$RMSE = \sqrt{\frac{1}{N} \sum_p \left| \log \mathcal{D}_p - \log \widehat{\mathcal{D}}_p \right|^2} \quad (9)$$

The Accuracy (Acc) as δ denotes the percentage of all pixels \mathcal{D}_p that satisfy max:

$$Acc = \left(\frac{\widehat{\mathcal{D}}_p}{\mathcal{D}_p}, \frac{\mathcal{D}_p}{\widehat{\mathcal{D}}_p} \right) < thr \quad (10)$$

where $thr = 1.25, 1.25^2, 1.25^3$.

4.4 Experiment Result

4.4.1 Qualitative and Quantitative Comparisons

Our experimental investigation encompasses both quantitative performance and energy consumption analyses, utilizing synthetic (DENSE) and real-world (DESC) datasets. A total of nine metrics were employed to evaluate the outcomes comprehensively.

	Abs Rel ↓	Sq Rel ↓	RMS log ↓	SI log ↓	$\delta < 1.25 \uparrow$	$\delta < 1.25^2 \uparrow$	$\delta < 1.25^3 \uparrow$	Spike-driven	Param (M)	Power (mJ)
U-Net	2.89	72.25	0.19	1.73	0.39	0.50	0.58	No	31.20	72.93
E2Depth	9.91	96.01	0.30	1.70	0.21	0.31	0.45	No	10.71	59.25
Spike-T	1.57	39.77	0.17	0.91	0.50	0.65	0.74	No	35.68	41.77
Proposed	0.80	8.32	0.17	0.46	0.53	0.68	0.76	Yes	20.55	12.43

Table 1. Quantitative performance comparison on the synthetic datasets (DENSE) using various models. Results for both the validation set and the test set are presented. Symbols ↓ and ↑ indicate that a lower value and higher value are preferable, respectively. The "Param" column refers to the number of parameters, and "Power" provides the average theoretical energy consumption for predicting an image.

Table 1 presents a quantitative performance comparison using synthetic datasets (specifically the DENSE dataset). The results consistently indicate that the proposed method outperforms the alternative approaches across nearly all evaluated metrics. Notably, significant enhancements are observed in the metrics of absolute relative error (Abs.Rel) and squared relative error (Sq.Rel). These are particularly critical metrics in depth estimation tasks. The Abs.Rel for the proposed method recorded at 0.80, significantly surpasses those of U-Net (2.89), E2Depth (9.91), and Spike-T (1.57), representing improvements of 72%, 91.9%, and 49% respectively. Similarly, the Sq.Rel of our method stands at 8.32, substantially lower than those of U-Net (72.25), E2Depth (96.01), and Spike-T (39.77), indicating improvements of 88.5%, 91.3%, and 79% respectively. Additionally, our method demonstrates marginal enhancements in accuracy metrics ($\delta < 1.25$, $\delta < 1.25^2$, and $\delta < 1.25^3$), achieving scores of 0.53, 0.68, and 0.76, respectively, which are slightly better than the competing methods.

In terms of power consumption, the proposed method, which leverages pure spike computing, shows a marked advantage over its competitors. Furthermore, the adoption of knowledge distillation has facilitated the use of merely four Transformer blocks in our method, significantly reducing the parameters compared to the Spike-T method, which utilizes eight Transformer blocks.

These experimental results show that our proposed method can more effectively capture the spatial-temporal characteristics of irregular continuous spike data streams, delivering satisfactory accuracy. This is further illustrated in Figure 8, which depicts the visualization results from multiple comparison models on a validation synthetic dataset. The visualization demonstrates that, unlike the U-Net and Spike-T methods which can predict details yet misestimate depth, or the E2Depth method that produces blurry outcomes losing fine details, our method effectively manages to capture more intricate details, including minute structures, sharp edges, and contours.

In addition, in order to validate the generalisability of the model, we evaluate the proposed model on DESC real event dataset and compare it with the three competing models (E2Depth, Spike-T and U-Net). It is noteworthy that while the DENSE synthetic dataset encompasses 128 spike frames, the real-world DESC dataset contains only 16 frames. Our model and the SpikeU-Net model require retraining on this reduced dataset. However, the SNN-based methods (E2Depth and Spike-T) are unable to be retrained due to insufficient training parameters, necessitating the replication of DESC data to 128 frames to accommodate their setups. Consequently, the performance of E2Depth and Spike-T are expectedly low.

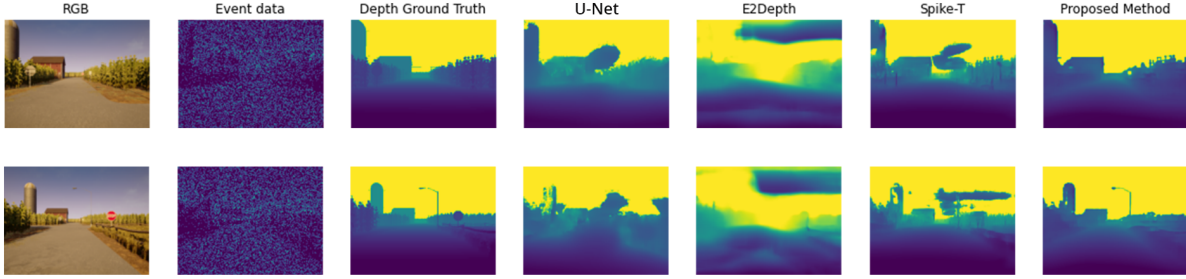


Figure 8. Visualization results of multiple comparison models on the synthetic (DENSE) dataset.

The results, as shown in Table 2, demonstrated that the proposed model excels across all metrics in comparison to the E2Depth, Spike-T, and U-Net models. This superior performance is evident particularly in terms of metrics such as Abs Rel, Sq Rel, RMS log, and SI log, as well as in the accuracy metrics ($\delta < 1.25$, $\delta < 1.25^2$, and $\delta < 1.25^3$), where higher scores are indicative of better performance. These findings underscore the effectiveness of the proposed model in handling real-event data from spiking cameras.

	Abs Rel ↓	Sq Rel ↓	RMS log ↓	SI log ↓	$\delta < 1.25$ ↑	$\delta < 1.25^2$ ↑	$\delta < 1.25^3$ ↑
E2Depth	9.909	96.011	0.299	1.697	0.209	0.309	0.448
Spike-T	2.853	51.757	0.321	0.751	0.164	0.341	0.483
SpikeU-Net	1.203	3.281	0.181	1.210	0.142	0.309	0.502
Proposed	1.000	0.999	0.105	0.212	0.387	0.500	0.583

Table 2. Quantitative comparison on the DESC real dataset.

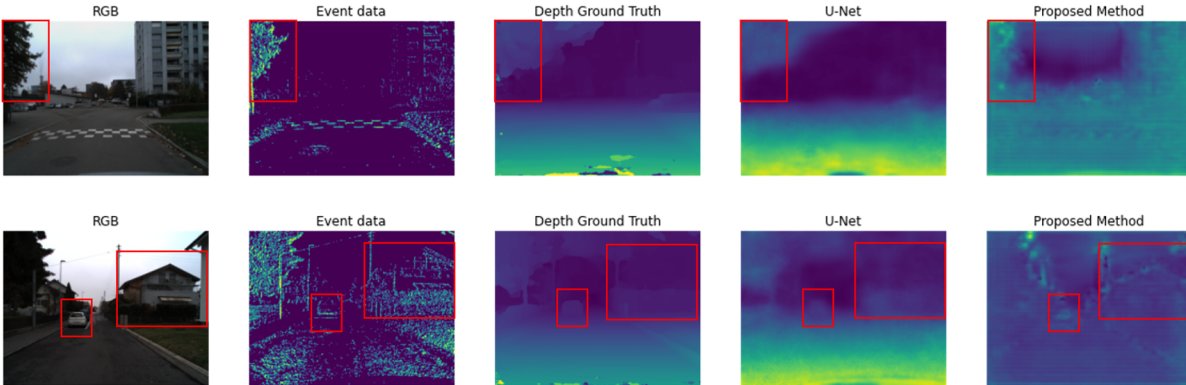


Figure 9. Visualization results under low-light conditions on the real(DESC) dataset.

Figure 9 shows the visualisation result in a low light environment. Our method effectively identifies features such as trees and houses along the roadside, as well as vehicles located in the center of the road.

4.4.2 Ablation study

This subsection presents an ablation study conducted to evaluate the effectiveness of the proposed Fusion Depth Estimation Head and Knowledge Distillation (KD) modules.

Table 3 reports the quantitative performance comparison on the synthetic datasets (DENSE) in the ablation study. As demonstrated by the results, all accuracy metrics exhibit a decline when employing the linear FCN (Fully Convolutional Network) head for depth estimation. Specifically, Absolute Relative (Abs Rel) error increased from 0.80 to 2.85, while the Squared Relative (Sq Rel) error escalated from 8.32 to 51.76. Figure 10 illustrates the visualization results of using two different heads. The image becomes notably blurrier and loses details when employing the linear FCN head, which relies solely on the

	Abs Rel ↓	Sq Rel ↓	RMS log ↓	SI log ↓	$\delta < 1.25 \uparrow$	$\delta < 1.25^2 \uparrow$	$\delta < 1.25^3 \uparrow$
Linear FCN Head	2.85	51.76	0.32	0.75	0.16	0.34	0.48
W/O KD	2.89	72.25	0.19	1.73	0.39	0.50	0.58
proposed	0.80	8.32	0.17	0.46	0.53	0.68	0.76

Table 3. Quantitative performance comparison on the synthetic (DENSE) dataset in the ablation study.

final features generated by the transformer. Conversely, our fusion head integrates multi-scale features, thereby facilitating superior recovery of details compared to the linear FCN head.

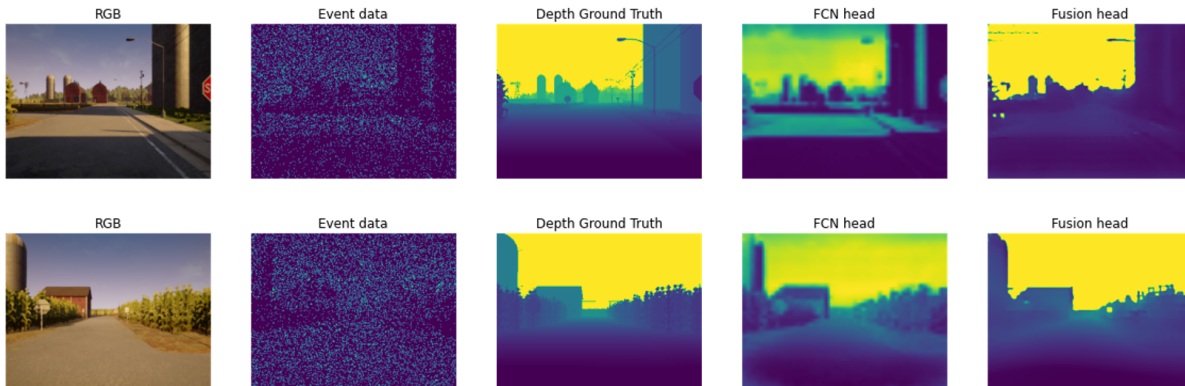


Figure 10. Visualization results on validation synthetic dataset by using fcn head and proposed fusion depth estimation head.

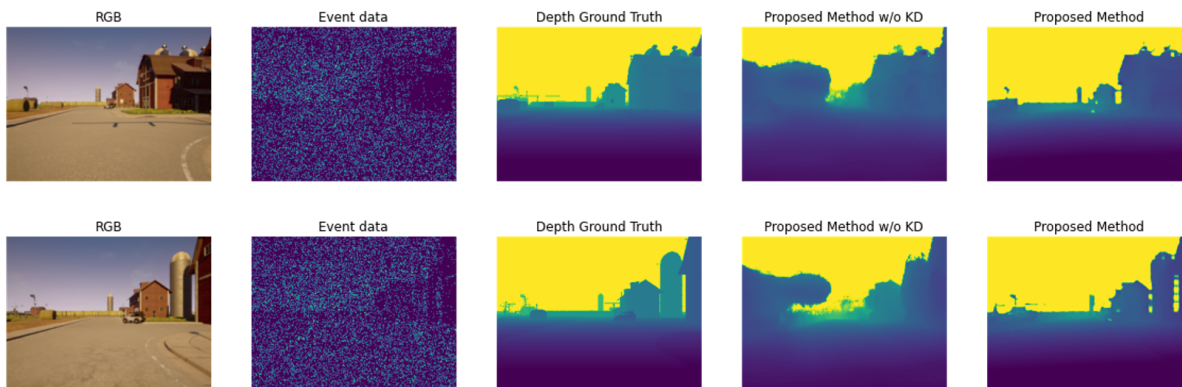


Figure 11. Visualization results on validation synthetic dataset with and without knowledge distillation.

The visualization of results with and without knowledge distillation is depicted in Figure 11. The results without knowledge distillation approximate TO those of the baseline models from Experiment 1. The presence of noise in the spike data leads to less accurate depth estimations for certain segments of the point cloud. However, employing knowledge distillation enables the model to predict the depths of distant clouds more accurately, a benefit attributed to the enhanced inductive capabilities derived from the substantial foundational model.

5 Conclusion

This paper presents a novel Spike Transformer network designed for depth estimation using data from spiking cameras. By integrating spike-driven residual learning and spiking self-attention mechanisms, we have developed a transformer architecture driven entirely by spikes. This design markedly increases the computational efficiency of Spiking Neural Networks (SNNs). Moreover, our single-stage knowledge transfer framework, which draws on large foundational ANN models such as DINO V2, enhances the performance of SNNs even with a limited data availability. Our experimental evaluations on both synthetic and real datasets demonstrate significant improvements across several metrics, notably in Abs Rel and Sq Rel (49% and

39.77% improvements over the state-of-the-art model Spike-T, respectively). In addition to its accuracy, the proposed model also exhibits lower power consumption, a critical attribute for practical applications. Future research will focus on further validation and deployment on real datasets and dedicated SNN processors, thus potentially broadening the applicability of Spike Transformers in real-world scenarios.

References

1. Gallego, G. *et al.* Event-based vision: A survey, DOI: [10.1109/TPAMI.2020.3008413](https://doi.org/10.1109/TPAMI.2020.3008413) (2022). Event-title: IEEE Transactions on Pattern Analysis and Machine Intelligence.
2. Tayarani-Najaran, M.-H. & Schmuker, M. Event-based sensing and signal processing in the visual, auditory, and olfactory domain: A review (2021). [Online; accessed 2023-08-15].
3. Chen, S. & Guo, M. Live demonstration: Celex-v: A 1m pixel multi-mode event-based sensor. 1682–1683, DOI: [10.1109/CVPRW.2019.00214](https://doi.org/10.1109/CVPRW.2019.00214) (2019). ISSN: 2160-7516.
4. Posch, C., Matolin, D. & Wohlgenannt, R. A qvga 143 db dynamic range frame-free pwm image sensor with lossless pixel-level video compression and time-domain cds, DOI: [10.1109/JSSC.2010.2085952](https://doi.org/10.1109/JSSC.2010.2085952) (2011). Event-title: IEEE Journal of Solid-State Circuits.
5. Furmonas, J., Liobe, J. & Barzdenas, V. Analytical review of event-based camera depth estimation methods and systems (2022). Publisher: MDPI.
6. Huang, X. *et al.* Real-time grasping strategies using event camera (2022). Publisher: Springer.
7. Cao, H., Chen, G., Xia, J., Zhuang, G. & Knoll, A. Fusion-based feature attention gate component for vehicle detection based on event camera (2021). Publisher: IEEE.
8. Chen, G. *et al.* Event-based neuromorphic vision for autonomous driving: A paradigm shift for bio-inspired visual sensing and perception, DOI: [10.1109/MSP.2020.2985815](https://doi.org/10.1109/MSP.2020.2985815) (2020). Event-title: IEEE Signal Processing Magazine.
9. Rafi, T. H. A brief review on spiking neural network-a biological inspiration (2021). Publisher: Preprints.
10. Lee, C. *et al.* Spike-flownet: Event-based optical flow estimation with energy-efficient hybrid neural networks. Lecture Notes in Computer Science, 366–382, DOI: [10.1007/978-3-030-58526-6_22](https://doi.org/10.1007/978-3-030-58526-6_22) (Springer International Publishing, Cham, 2020).
11. Auge, D., Hille, J., Mueller, E. & Knoll, A. A survey of encoding techniques for signal processing in spiking neural networks, DOI: [10.1007/s11063-021-10562-2](https://doi.org/10.1007/s11063-021-10562-2) (2021).
12. Cordone, L., Miramond, B. & Ferrante, S. Learning from event cameras with sparse spiking convolutional neural networks. 1–8, DOI: [10.1109/IJCNN52387.2021.9533514](https://doi.org/10.1109/IJCNN52387.2021.9533514) (2021). ISSN: 2161-4407.
13. Zhao, C., Sun, Q., Zhang, C., Tang, Y. & Qian, F. Monocular depth estimation based on deep learning: An overview, DOI: [10.1007/s11431-020-1582-8](https://doi.org/10.1007/s11431-020-1582-8) (2020).
14. Ming, Y., Meng, X., Fan, C. & Yu, H. Deep learning for monocular depth estimation: A review, DOI: [10.1016/j.neucom.2020.12.089](https://doi.org/10.1016/j.neucom.2020.12.089) (2021).
15. Laga, H., Jospin, L. V., Boussaid, F. & Bennamoun, M. A survey on deep learning techniques for stereo-based depth estimation, DOI: [10.1109/TPAMI.2020.3032602](https://doi.org/10.1109/TPAMI.2020.3032602) (2022). Event-title: IEEE Transactions on Pattern Analysis and Machine Intelligence.
16. Fang, W. *et al.* Deep residual learning in spiking neural networks. vol. 34, 21056–21069 (Curran Associates, Inc., 2021). [Online; accessed 2023-08-15].
17. Hu, Y., Tang, H. & Pan, G. Spiking deep residual networks, DOI: [10.1109/TNNLS.2021.3119238](https://doi.org/10.1109/TNNLS.2021.3119238) (2023). Event-title: IEEE Transactions on Neural Networks and Learning Systems.
18. Yin, B., Corradi, F. & Bohté, S. M. Effective and efficient computation with multiple-timescale spiking recurrent neural networks. ICONS 2020, 1–8, DOI: [10.1145/3407197.3407225](https://doi.org/10.1145/3407197.3407225) (Association for Computing Machinery, New York, NY, USA, 2020). [Online; accessed 2023-08-15].
19. Diehl, P. U., Zarella, G., Cassidy, A., Pedroni, B. U. & Neftci, E. Conversion of artificial recurrent neural networks to spiking neural networks for low-power neuromorphic hardware. 1–8, DOI: [10.1109/ICRC.2016.7738691](https://doi.org/10.1109/ICRC.2016.7738691) (2016).
20. Dosovitskiy, A. *et al.* An image is worth 16x16 words: Transformers for image recognition at scale (2020). ArXiv: 2010.11929.

21. Han, K. *et al.* A survey on vision transformer, DOI: [10.1109/TPAMI.2022.3152247](https://doi.org/10.1109/TPAMI.2022.3152247) (2023). Event-title: IEEE Transactions on Pattern Analysis and Machine Intelligence.
22. Liu, Z. *et al.* Swin transformer: Hierarchical vision transformer using shifted windows (2021). ArXiv: 2103.14030.
23. Sun, Z., Cao, S., Yang, Y. & Kitani, K. M. Rethinking transformer-based set prediction for object detection. 3611–3620 (2021). [Online; accessed 2023-08-15].
24. Yang, J., An, L., Dixit, A., Koo, J. & Park, S. I. Depth estimation with simplified transformer, DOI: [10.48550/arXiv.2204.13791](https://doi.org/10.48550/arXiv.2204.13791) (2022). ArXiv:2204.13791 [cs].
25. Zhao, C. *et al.* Monovit: Self-supervised monocular depth estimation with a vision transformer. 668–678, DOI: [10.1109/3DV57658.2022.00077](https://doi.org/10.1109/3DV57658.2022.00077) (2022). ISSN: 2475-7888.
26. Zhang, J., Tang, L., Yu, Z., Lu, J. & Huang, T. Spike transformer: Monocular depth estimation for spiking camera. In *European Conference on Computer Vision*, 34–52 (Springer, 2022).
27. Zhou, Z. *et al.* Spikformer: When spiking neural network meets transformer, DOI: [10.48550/arXiv.2209.15425](https://doi.org/10.48550/arXiv.2209.15425) (2022). ArXiv:2209.15425 [cs].
28. Zhou, C. *et al.* Spikingformer: Spike-driven residual learning for transformer-based spiking neural network (2023). ArXiv:2304.11954 [cs].
29. He, X. *et al.* Improving the performance of spiking neural networks on event-based datasets with knowledge transfer (2023). ArXiv:2303.13077 [cs].
30. Oquab, M. *et al.* Dinov2: Learning robust visual features without supervision, DOI: [10.48550/arXiv.2304.07193](https://doi.org/10.48550/arXiv.2304.07193) (2023). ArXiv:2304.07193 [cs].
31. Ranftl, R., Lasinger, K., Hafner, D., Schindler, K. & Koltun, V. Towards robust monocular depth estimation: Mixing datasets for zero-shot cross-dataset transfer, DOI: [10.48550/arXiv.1907.01341](https://doi.org/10.48550/arXiv.1907.01341) (2020). ArXiv:1907.01341 [cs].
32. Ranftl, R., Bochkovskiy, A. & Koltun, V. Vision transformers for dense prediction (2021). ArXiv:2103.13413 [cs].
33. Hidalgo-Carrió, J., Gehrig, D. & Scaramuzza, D. Learning monocular dense depth from events (2020). ArXiv:2010.08350 [cs].
34. Khan, F., Salahuddin, S. & Javidnia, H. Deep learning-based monocular depth estimation methods—a state-of-the-art review, DOI: [10.3390/s20082272](https://doi.org/10.3390/s20082272) (2020). Number: 8 publisher: Multidisciplinary Digital Publishing Institute.
35. Li, Q. *et al.* Deep learning based monocular depth prediction: Datasets, methods and applications, DOI: [10.48550/arXiv.2011.04123](https://doi.org/10.48550/arXiv.2011.04123) (2020). ArXiv:2011.04123 [cs].
36. Laina, I., Rupprecht, C., Belagiannis, V., Tombari, F. & Navab, N. Deeper depth prediction with fully convolutional residual networks (2016). ArXiv:1606.00373 [cs] version: 2.
37. Ronneberger, O., Fischer, P. & Brox, T. U-net: Convolutional networks for biomedical image segmentation. 234–241 (2015).
38. Nam, Y., Mostafavi, M., Yoon, K.-J. & Choi, J. Stereo depth from events cameras: Concentrate and focus on the future. 6104–6113, DOI: [10.1109/CVPR52688.2022.00602](https://doi.org/10.1109/CVPR52688.2022.00602) (IEEE, New Orleans, LA, USA, 2022). [Online; accessed 2023-08-18].
39. Liu, X., Li, J., Fan, X. & Tian, Y. Event-based monocular dense depth estimation with recurrent transformers (2022). ArXiv:2212.02791 [cs].
40. Liu, J. *et al.* Unsupervised spike depth estimation via cross-modality cross-domain knowledge transfer, DOI: [10.48550/arXiv.2208.12527](https://doi.org/10.48550/arXiv.2208.12527) (2022). ArXiv:2208.12527 [cs].
41. Hodgkin, A. L. & Huxley, A. F. A quantitative description of membrane current and its application to conduction and excitation in nerve (1952). Publisher: Wiley-Blackwell.
42. Izhikevich, E. M. Simple model of spiking neurons (2003). Publisher: IEEE.
43. Zheng, H., Wu, Y., Deng, L., Hu, Y. & Li, G. Going deeper with directly-trained larger spiking neural networks, DOI: [10.48550/arXiv.2011.05280](https://doi.org/10.48550/arXiv.2011.05280) (2020). ArXiv:2011.05280 [cs].
44. Yao, M. *et al.* Spike-driven transformer, DOI: [10.48550/arXiv.2307.01694](https://doi.org/10.48550/arXiv.2307.01694) (2023). ArXiv:2307.01694 [cs].
45. Gou, J., Yu, B., Maybank, S. J. & Tao, D. Knowledge distillation: A survey (2021). ArXiv: 2006.05525.
46. Kushawaha, R. K., Kumar, S., Banerjee, B. & Velmurugan, R. Distilling spikes: Knowledge distillation in spiking neural networks, DOI: [10.48550/arXiv.2005.00288](https://doi.org/10.48550/arXiv.2005.00288) (2020). ArXiv:2005.00288 [cs].

47. Qiu, H. *et al.* Self-architectural knowledge distillation for spiking neural networks (2022). [Online; accessed 2023-08-22].
48. Bommasani, R. *et al.* On the opportunities and risks of foundation models, DOI: [10.48550/arXiv.2108.07258](https://doi.org/10.48550/arXiv.2108.07258) (2022). ArXiv:2108.07258 [cs].
49. Fan, H. *et al.* Multiscale vision transformers, DOI: [10.48550/arXiv.2104.11227](https://doi.org/10.48550/arXiv.2104.11227) (2021). ArXiv:2104.11227 [cs].
50. Wang, W. *et al.* Pyramid vision transformer: A versatile backbone for dense prediction without convolutions (2021). [Online; accessed 2021-05-06].
51. Lee, Y., Kim, J., Willette, J. & Hwang, S. J. Mpvit: Multi-path vision transformer for dense prediction, DOI: [10.48550/arXiv.2112.11010](https://doi.org/10.48550/arXiv.2112.11010) (2021). ArXiv:2112.11010 [cs].
52. Johnson, J., Alahi, A. & Fei-Fei, L. Perceptual losses for real-time style transfer and super-resolution. In *Computer Vision—ECCV 2016: 14th European Conference, Amsterdam, The Netherlands, October 11–14, 2016, Proceedings, Part II 14*, 694–711 (Springer, 2016).
53. Eigen, D. & Fergus, R. Predicting depth, surface normals and semantic labels with a common multi-scale convolutional architecture, DOI: [10.48550/arXiv.1411.4734](https://doi.org/10.48550/arXiv.1411.4734) (2015). ArXiv:1411.4734 [cs].

Acknowledgements (not compulsory)

This work is supported by the BBSRC (Projects BB/R019983/1, BB/S020969/1 and EP/X013707/1).

Author contributions statement

Xin Zhang and Liangxiu Han conceived the experiment(s), Xin Zhang and Tam Sobeih conducted the experiment(s), Xin Zhang and Tam Sobeih analysed the results. All authors reviewed the manuscript.